Progress In Electromagnetics Research C, Vol. 49, 105–113, 2014

A Family of Directive Metamaterial-Inspired Antennas

Saber Dakhli[1, 2], Hatem Rmili[3, *], Kouroch Mahdjoubi[4], Jean-Marie Floc'h[2], and Fethi Choubani[1]

Abstract—A new family of metamaterial-inspired monopole antennas designed for GPS operation is reported. By adding a simple Split-Ring Resonator (SRR) into the near-field region of a monopole antenna resonating at 2.45 GHz, we have created a second resonance situated in the L1-band ($f = 1,537$ for example) lower than the monopole's one. At this new resonance, the directivity of the structure was enhanced and its profile was reduced. Four SRR-configurations were considered depending on the orientation of the slot into the resonator. The structure was first optimized by adjusting the resonator size and the coupling distance between it and the monopole. Next, the directivity of the structure was improved by adjusting both the SRR-slot position and the coupling distance. Finally, the optimized structure in terms of size and directivity was realized and characterized.

1. INTRODUCTION

The rapid progress of wireless devices for communication has increased the requirement of efficient, low profile, light weight and low cost electrically small antennas (ESAs). To satisfy this trend, a variety of antennas have been engineered with metamaterials (MTMs) [1] and metamaterial-inspired constructs [2, 3] in order to improve their performances such as miniaturization [4–7], high efficiency [8–10], enhanced bandwidth [11, 12], high gain [13, 14], and reconfigurability [15, 16].

The concept of metamaterial-inspired antenna was proposed first in 2007 by Ziolkowski for the design of an efficient and electrically-small antenna system operating at multi-frequency bands [17]. This concept is based on the fact that the resistive and reactance antenna matching is achieved not with a metamaterial (spherical shell) medium but rather with an element such as an inclusion that has or could be used in a metamaterial unit cell design to realize an epsilon-negative (ENG), mu-negative (MNG), or double-negative (DNG) medium.

In fact, the added single metamaterial cell brings some complementary impedance to the principal (monopole) antenna to match the antenna at a lower frequency and then miniaturizes the structure size, to increase the efficiency, bandwidth ... etc. Recently, it is shown that these structures are also capable to increase the directivity [18–20].

In this paper, we use, as metamaterial cell, a simple Split-Ring Resonator (SRR) cell in which we change the position of the slot, which has an additional parameter for the control of the radiation pattern shape, and then the improvement of the directivity. Therefore, four configurations of the structure are considered corresponding to the four orientations of the slot.

Details of the structure design and simulated return loss are given in Section 2. In Section 3, we study the effect of the resonator dimensions and the coupling distance on the size of the antenna. Section 4 presents the effect of both the SRR-slot orientation and the coupling distance on the directivity of the structure. In Section 4, the impedance matching and radiation properties of the optimized

Received 5 March 2014, Accepted 11 April 2014, Scheduled 18 April 2014

* Corresponding author: Hatem Rmili (hmrmili@kau.edu.sa).

[1] Innov'Com Laboratory, SUPCOM, University of Carthage, Tunis, Tunisia. [2] IETR, University of Rennes 1, Campus Beaulieu — bât.11D, #263, Av. Général Leclerc, CS 74205, Rennes Cedex 35042, France. [3] Electrical and Computer Engineering Department, King Abdulaziz University, P. O. Box 80204, Jeddah 21589, Saudi Arabia. [4] IETR, INSA, 20 avenue buttes des coësmes, Rennes 35043, France.

structure are presented and compared to simulated results. Finally, Section 5 gives the main concluded results.

2. ANTENNAS DESIGN

As shown in Figure 1, the proposed structure consists of both a monopole and a SRR printed on a Rogers Duroid^{TM} 5880 substrate of thickness $h = 0.8\,\text{mm}$ and relative permittivity $\varepsilon_r = 2.2$, and mounted orthogonally on a rectangular ground plane of dimensions $200 \times 200\,\text{mm}^2$.

The printed monopole of length L_M and width W_M is coupled electromagnetically with a rectangular SRR element of exterior dimensions $L_R \times W_R$, width t and gap W_g. The coupling distance between the monopole and the resonator is denoted d_1, whereas the distance separating the ground plane to the lower edge of the SRR is d_2. Details on the parameters design are given in Figure 2(a) and Table 1.

We have studied four antennas A1, A2, A3 and A4 by considering different configurations of the SRR cell depending on the slot location (Figure 2).

The design procedure starts with the optimization of the planar monopole length L_M to adjust the resonant frequency of the monopole at $F_M = 2.45\,\text{GHz}$ (see Figure 3). This goal was easily achieved by taking $L_M = 26\,\text{mm}$, which corresponds to a quarter-wavelength resonance ($L_M \approx \lambda_{eff}/4$). λ_{eff} is the effective wavelength in the propagating medium. Then, by adding a rectangular SRR element of

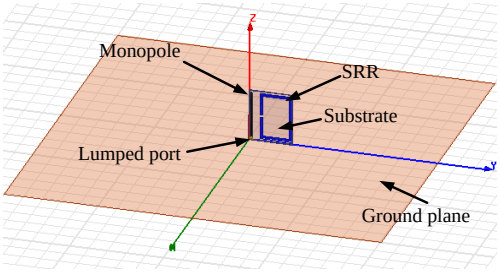

Figure 1. Schema of the proposed antenna.

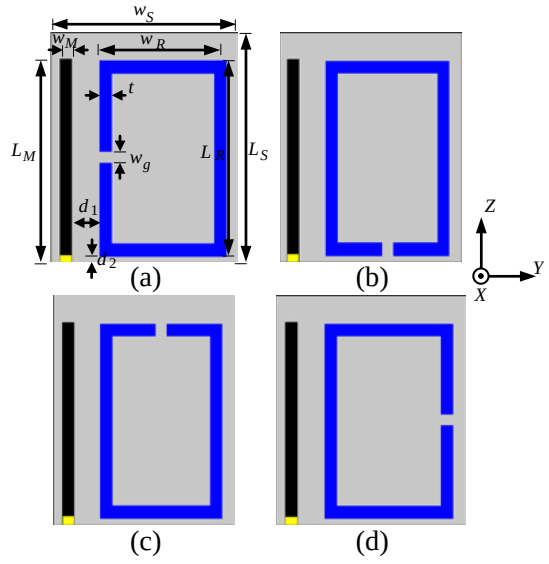

Figure 2. The four studied antennas with different configurations of the SRR-slot: (a): A1; (b): A2; (c): A3; and (d): A4.

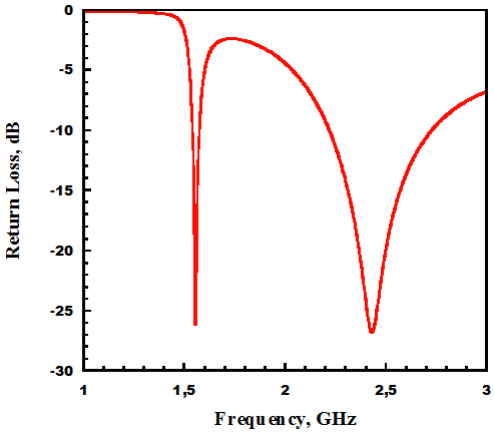

Figure 3. Simulated return loss of antenna A1 showing the monopole resonance at $F_M = 2.45\,\text{GHz}$, and the SRR resonance at $F_R = 1.55\,\text{GHz}$.

Table 1. Parameters design of the A1 antenna configuration.

Dimensions in mm			
Parameters	**Values**	**Parameters**	**Values**
$\boldsymbol{L_S}$	30	$\boldsymbol{W_R}$	17
$\boldsymbol{W_S}$	23	$\boldsymbol{t}$	1.5
$\boldsymbol{L_M}$	26	$\boldsymbol{W_g}$	1.5
$\boldsymbol{W_M}$	1.5	$\boldsymbol{d_1}$	4
$\boldsymbol{L_R}$	25	$\boldsymbol{d_2}$	1

dimensions $L_R \times W_R$, we have created a parasitic resonance at $F_R = 1.55\,\text{GHz}$ which is lower than the monopole resonance F_M.

In fact, at frequencies lower than F_M, the monopole is not resonating, but acting as a feed element for the SRR cell which resonates at the frequency F_R ($F_R < F_M$). The frequency F_R of the SRR-cell corresponds to a half-wave length ($\lambda_{eff}/2$) resonance with a resonant current path L_{res} given by:

$$L_{res} = 2(L_R + W_R) \approx \frac{\lambda_{eff}}{2} \tag{1}$$

The dispersion relation is as follows [21]:

$$k = \frac{\omega_{\text{LC}}}{c} \tag{2}$$

where

$$\omega_{\text{LC}} \approx \frac{1}{(L_{Res}/4)} \frac{c}{\varepsilon_c} \sqrt{\frac{w_g}{t}} \tag{3}$$

ε_c is the permittivity of the conducting material (copper), and ω_{LC} is the pulsation related LC circuit used to model the square resonator.

Consequently, the resonance frequency F_R can be approximated by:

$$F_R \approx \frac{C}{4(L_R + W_R)\sqrt{\varepsilon_{eff}}} \tag{4}$$

where k is the wave number, c the velocity of light in free space, and ε_{eff} the effective permittivity of the substrate ($\varepsilon_{eff} \approx 1.3$).

3. MINIATURIZATION OF THE STRUCTURE

It is shown in the previous section that the presence of an SRR element close to the monopole creates a new resonant frequency lower than the monopole one, which allows the miniaturization of the structure. In fact, two main parameters are controlling the frequency shift of F_R towards lower frequencies: the size of the rectangular resonator (L_R and W_R), and the coupling distance d_1 between the monopole and the resonator. In this section, these parameters are studied in order to achieve the lowest operating frequency, and then reduce the antenna size.

3.1. Effect of the SRR-size

The influence of the SRR-size on the lowest resonant frequency is investigated by studying the effects of the length L_R and width W_R of the resonator on the impedance matching of antenna A1 as shown in Figure 4.

Since the resonance F_R is depending especially on the resonator size (see Eq. (2)) and not the slot position, we have limited our study to configuration A1.

The SRR-monopole spacing is fixed to $d_1 = 4\,\text{mm}$. The parameters W_R and L_R are varied, but they still inferior to the monopole height L_M in order to reduce the size of the structure.

We can notice from Figure 4 that by increasing the loop dimensions L_R and W_R, the resonant frequency F_R shifts toward low frequencies allowing the reduction of the antenna size. This result can be justified directly by Formula (2). Hence, the lowest matched frequency ($F_R = 1.537\,\text{GHz}$) is obtained for the length $L_R = 25\,\text{mm}$ and the width $W_R = 17\,\text{mm}$.

3.2. Effect of the Coupling Distance

After optimizing the resonator size, we have studied the effect of the distance separating the resonator from the monopole in order to decrease further the frequency F_R and then decrease the structure size.

The coupling distance between the resonator and the monopole, and the slot position highly affect the monopole resonance F_R. Figure 5 gives the simulated return loss of the antenna A1 for different values of the coupling distance d_1. It is found that the distance $d_1 = 4\,\text{mm}$ gives the best impedance matching for the structure A1 ($S_{11} = -25.2\,\text{dB}$ at $F_R = 1.537\,\text{GHz}$). In fact, at this frequency, the monopole brings capacitive impedance to the SRR which behaves as an inductive element.

The presence of the SRR element allows the compensation of the monopole reactive impedance for better impedance matching of the antenna.

We have also determined the optimum coupling distance giving the best impedance matching for

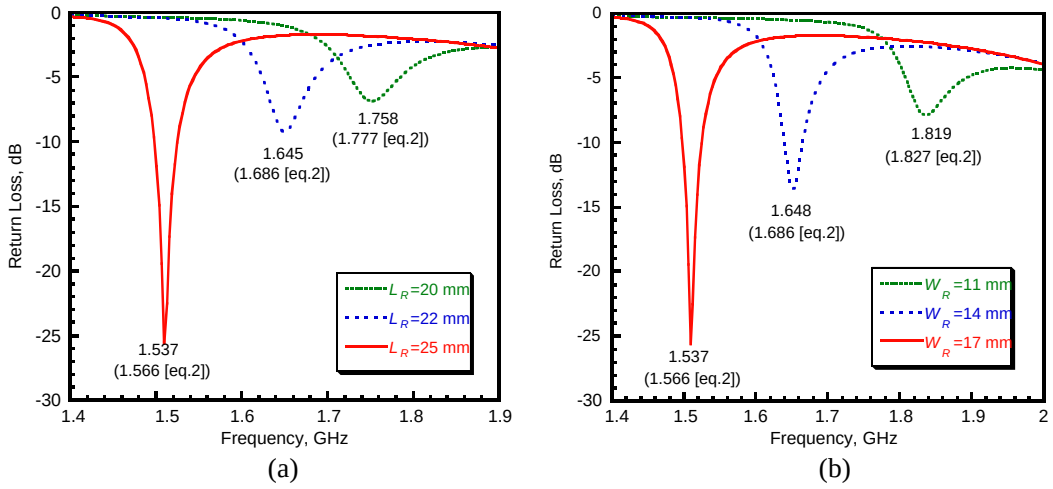

Figure 4. Simulated return loss of antenna A1 for different values of the SRR (a) length L_R and (b) width W_R.

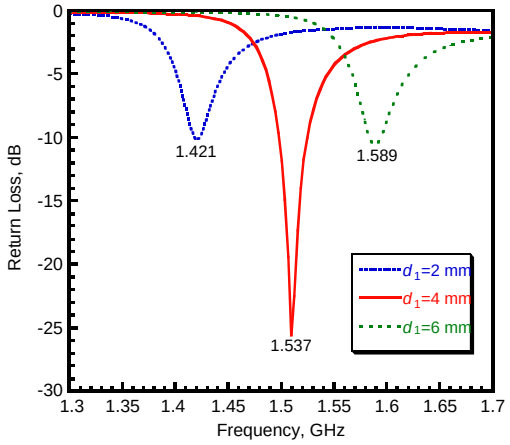

Figure 5. Simulated return loss of the antenna A1 for different values of the distance d_1.

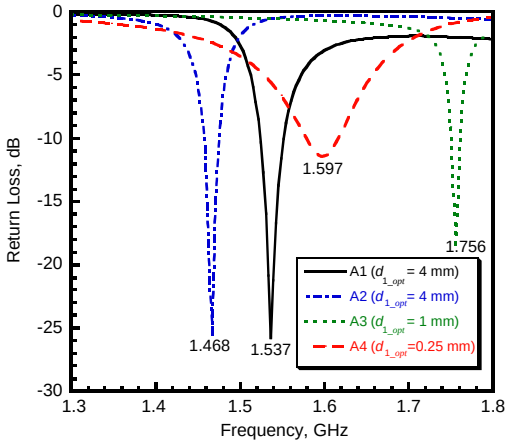

Figure 6. Simulated return loss for the four antenna configurations.

the other configurations A2, A3 and A4. Figure 6 shows the evolution of the simulated return loss for all the configurations A1–A4 versus the frequency by taking, for each one, the optimum coupling distance d_1.

We can notice from Figure 6 and Table 2 that configurations A1 and A2 give the best impedance matching. However, configuration A2 is more compact than A1.

4. OPTIMIZATION OF THE DIRECTIVITY

The numerical analysis of the structure shows that the directivity is highly influenced by the SRR-slot orientation and coupling distance. These parameters are then studied and optimized in order to increase the antenna directivity.

4.1. Effect of the Slot Position

Figure 7 illustrates simulated surface current and 3D radiation patterns at the resonant frequencies F_R for the configurations A1–A4.

We can observe a directive radiation behavior for both antennas A1 and A3, where a directive beam toward the negative y-direction is reported for configuration A1, and toward the positive Y-direction for configuration A3. We can also notice that antenna A2 presents two radiation directions along the y-axis, whereas antenna A4 behaves as a monopole placed along the z-axis, with low directivity.

By analyzing the surface current distribution at the lower frequency F_R, we can notice that maximum currents are localized basically in the resonator, which means that only the resonator is excited at this frequency.

4.2. Effect of the Coupling Distance

The directivity and the gain versus the coupling distance d_1 are shown in Figure 8, for all the configurations A1–A4.

We can notice from Figure 8 that configurations A1 and A3 may produce a maximum directivity of 8.33 dB and 9.48 dB, respectively, which can be qualified as superdirectivity regarding the size of these antennas. Whereas for configurations A2 and A4, the directivity is much lower (5.5 for A2 and 6 dB for A4). Concerning the gain (dashed curves in Figure 8), it attains a maximum value for the distance d_{1_opt} (see Table 2) and then falls down rapidly. The reason for this gain drop is the mismatching of the antenna for distances different to d_{1_opt} (see Figure 6).

The antenna efficiency seems to be less dependent on the coupling distance than the gain. We can notice from Figure 8 that the efficiency also attains a maximum value for a certain coupling distance, which is different from d_{1_opt}, then decreases slowly, and becomes poor due to the high value of the return loss.

We should mention here that if the antennas are matched again by adding external matching circuits, the gain will be improved and even can attain the value of the directivity if the efficiency of the matching circuit is good.

Table 2. Results of the four proposed configurations.

	d_{1_opt} (mm)	F_R (MHz)	ka
A1 antenna	4	1.537	0.61
A2 antenna	4	1.468	0.58
A3 antenna	1	1.756	0.69
A4 antenna	0.25	1.597	0.63

a is the radius of the smallest hemisphere enclosing the antenna,
and $k = 2\pi/\lambda_{res}$ is the wave number in free space at the resonance frequency.

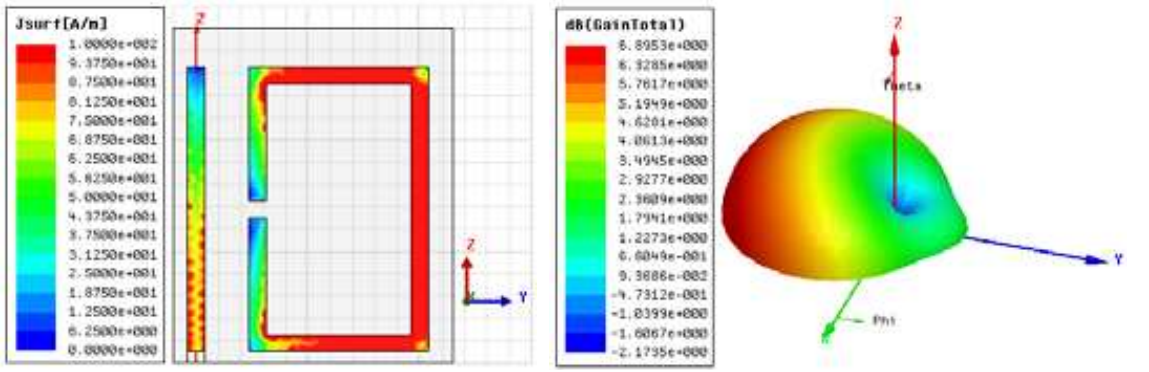

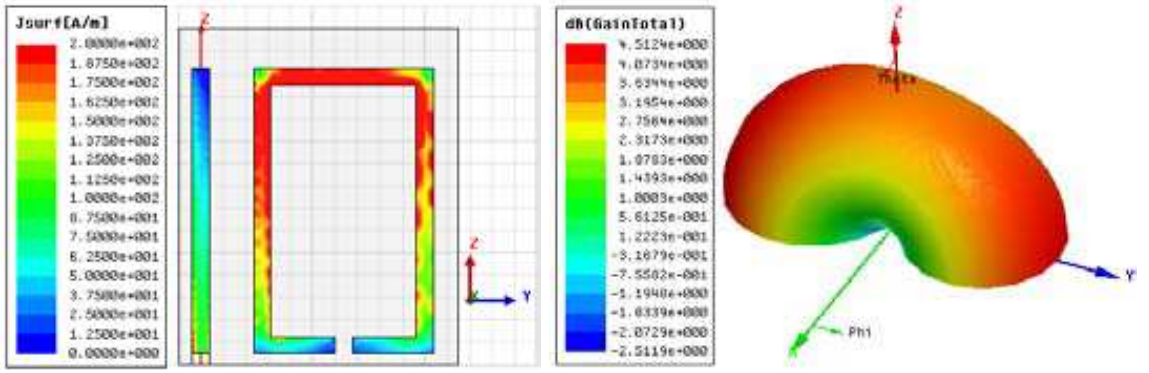

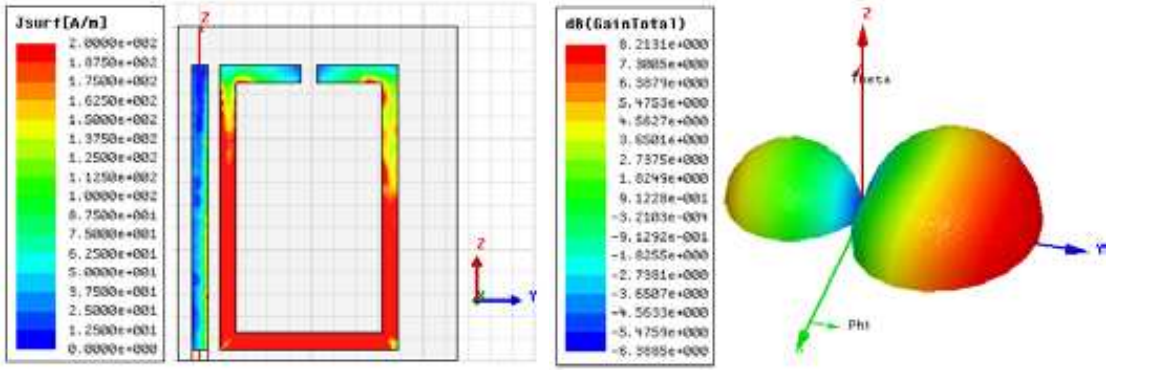

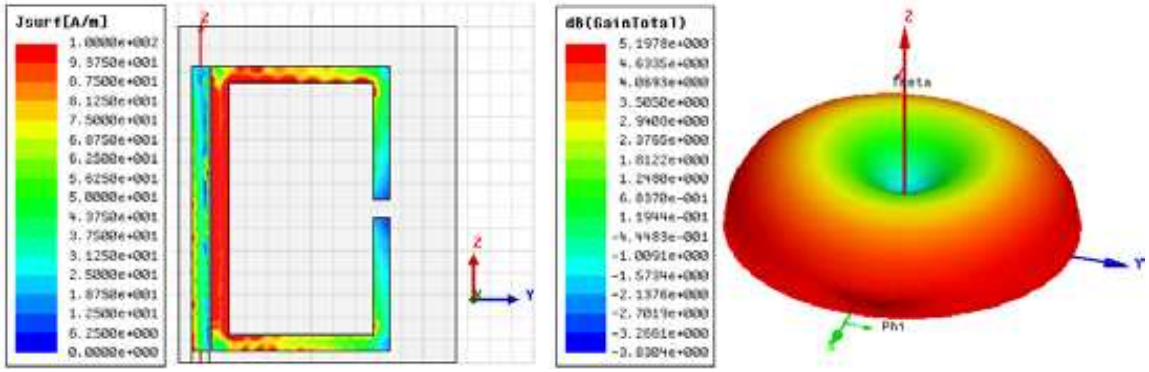

Figure 7. Simulated surface currents and radiation patterns, at the frequency F_R, of the proposed structure for all the configurations A1–A4.

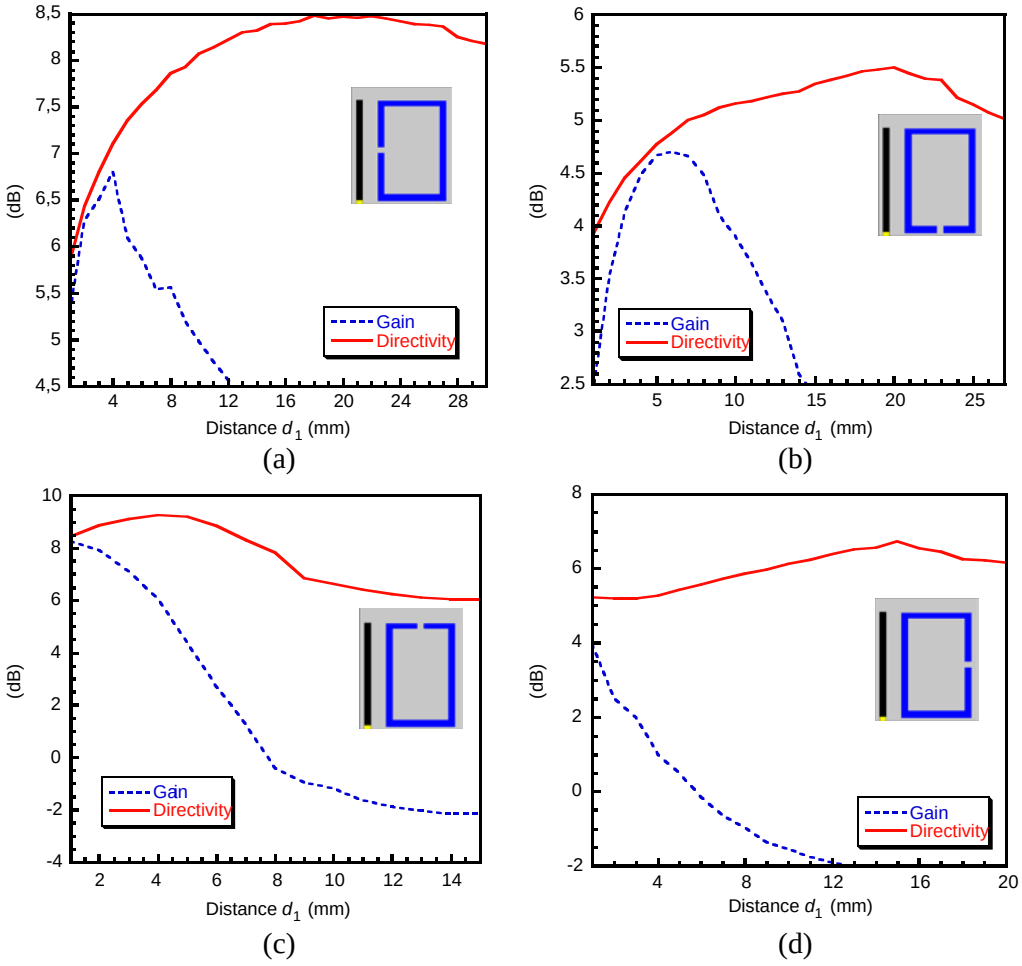

Figure 8. Simulated gain and directivity versus the coupling distance d_1 for the configurations: (a) A1; (b) A2; (c) A3; and (d) A4.

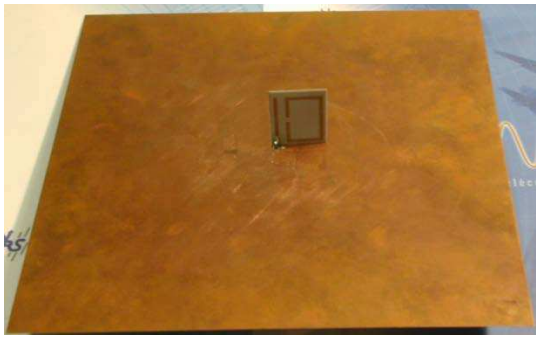

Figure 9. Photo of the realized prototype (Antenna A1).

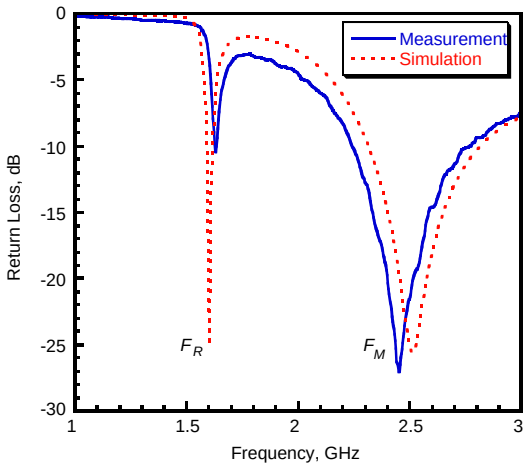

Figure 10. Simulated and measured return loss for the optimized antenna A1.

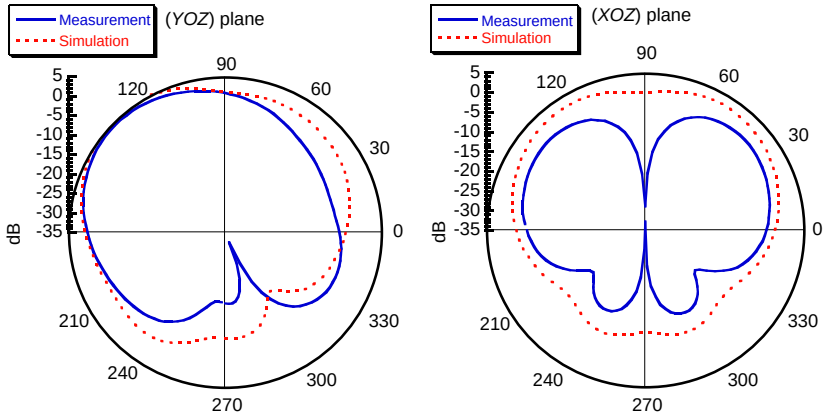

Figure 11. Simulated and measured radiation patterns in (XOZ) and (YOZ) planes of the A1 antenna at the frequency F_R.

5. CHARACTERIZATION OF THE OPTIMIZED PROTOTYPE A1

After the optimization procedure of the resonator size, coupling distance and slot-orientation, we have realized the best structure in terms of compactness and directivity, which corresponds to configuration A1. The final prototype ($L_R = 25\,\text{mm}$, $W_R = 17\,\text{mm}$ and $d_1 = 4\,\text{mm}$) is shown in Figure 9.

The impedance matching of antenna A1 (Figure 10) was investigated over the frequency range 1–3 GHz by using the network analyzer Agilent N5230A. From Figure 10, We can notice a good agreement between simulation and measurements.

Measurements on the radiation patterns of antenna A1 were carried out in the anechoic chamber "SATIMO Stargate32" at the IETR Institute. Figure 11 illustrates simulated and measured radiation patterns in both (xz) and (yz) planes. We should mention here that the results correspond to the realized version (Figure 9), where the ground plane has finite size. Good agreement between numerical and experimental results is obtained especially for the yz plane. The maximum measured gain at $d_1 = 4\,\text{mm}$ is 4.28 dB, while the simulated gain is 6.8 dB (see Figure 8).

The difference between simulation and measurement may be attributed to the finite size of the ground plane used for the antenna prototype.

6. CONCLUSION

In this work, a super directive metamaterial-inspired antenna is designed for GPS systems operating in L1-band. The structure is composed of printed monopole and SRR elements mounted orthogonally on a finite ground plane.

Four configurations (A1–A4) depending on the position of the SRR-slot are studied. It is found that the slot position and coupling distance are two main parameters for the optimization of the size and the directivity of the structure. For the optimized configuration denoted A1, we have obtained a good compactness ($ka = 0.61$) and directivity (8.88 dB) at the operating frequency 1.537 GHz.

ACKNOWLEDGMENT

The authors wish to acknowledge the DSR (Deanship of Scientific Research) of the King Abdulaziz University, Jeddah, Saudi Arabia, for their financial support.

REFERENCES

1. Engheta, N. and R. W. Ziolkowski (eds.), *Metamaterials: Physics and Engineering Explorations,* IEEE Press, Wiley Publishing, 2006.

2. Ziolkowski, R. W., P. Jin, and C.-C. Lin, "Metamaterial-inspired engineering of antennas," *Proceeding of IEEE*, Vol. 57, 2548–2563, Oct. 2011.
3. Erentok, A. and R. W. Ziolkowski, "Metamaterial-inspired efficient electrically small antennas," *IEEE Transactions on Antennas and Propagation*, Vol. 56, No. 3, 691–707, Mar. 2008.
4. Jin, P. and R. W. Ziolkowski, "Broadband, efficient, electrically small antennas facilitated by active near-field resonant parasitic elments," *IEEE Transactions on Antennas and Propagation*, Vol. 58, No. 2, 318–327, Feb. 2010.
5. Dakhli, S., K. Mahdjoubi, H. Rmili, J. M. Floc'h, and H. Zangar, "Compact, multifunctional, metamaterial-inspired monopole antenna," *European Conference on Antennas and Propagation, EUCAP*, 1967–1970, Prague, Czech Republic, Mar. 2012.
6. Dakhli, S., J. M. Floc'h, K. Mahdjoubi, H. Rmili, and H. Zangar, "Compact and multi-band metamaterial-inspired dipole antenna," *European Conference on Antennas and Propagation, EUCAP*, 2765–2768, Gothenburg, Sweden, Apr. 2013.
7. Goncalves, R., N. B. Carvalho, and P. Pinho, "Metamaterial inspired compact printed antenna for WLAN applications," *IEEE Antennas and Propagation Society International Symposium (APS-URSI)*, 1382–1383, 2013.
8. Erentok, A. and R. W. Ziolkowski, "A dual-band efficient metamaterial-inspired electrically-small magnetic-based antenna," *IEEE Antennas and Propagation Society International Symposium*, 1877–1880, 2007.
9. Jin, P. and R. W. Ziolkowski, "Low-Q, electrically small, efficient near-field resonant parasitic antennas," *IEEE Transactions on Antennas and Propagation*, Vol. 57, No. 9, 2548–2563, Sep. 2009.
10. Dakhli, S., K. Mahdjoubi, J. M. Floc'h, H. Rmili, and H. Zangar, "Efficient, metamaterial-inspired loop-monopole antenna with shaped radiation pattern," *Loughborough Antenna and Propagation Conference, LAPC*, 1–4, Loughborough, England, Nov. 2012.
11. Nordin, M. A. and M. T. Islam, "A bandwidth enhanced printed dipole antenna with metamaterial-inspired loading," *IEEE International Conference on Space Science and Communication (IconSpace)*, 183–185, Melaka, Malaysia, Jul. 2013.
12. Majedi, M. S. and A. R. Attari, "A compact and broadband metamaterial-inspired antenna," *IEEE Antennas and Wireless Propagation Letters*, Vol. 12, 345–348, Jun. 2013.
13. Zhu, N., Q. Feng, and Q. Xiang, "Metamaterial-inspired high-gain array antenna," *Cross Strait Quad-Regional Radio Science and Wireless Technology Conference (CSQRWC)*, 375–378, 2011.
14. Yaghjian, A. D., "Increasing the supergain of electrically small low antennas using metamaterials," *European Conference on Antennas and Propagation, EUCAP*, 151–155, Gothenburg, Sweden, Apr. 2010.
15. Mirzaei, H. and G. Eleftheriades, "A compact frequency-reconfigurable metamaterial-inspired antenna," *IEEE Antennas and Wireless Propagation Letters*, Vol. 10, 1154–1157, Jun. 2011.
16. Turkmen, O., G. Turhan-Sayan, and R. W. Ziolkowski, "Metamaterial inspired, electrically small, GSM antenna with steerable radiation patterns and high radiation efficiency," *IEEE Antennas and Propagation Society International Symposium (APS-URSI)*, 770–771, 2013.
17. Erentok, A. and R. W. Ziolkowski, "A dual-band efficient metamaterial-inspired electrically-small magnetic-based antenna," *IEEE Antennas and Propagation Society International Symposium (APS-URSI)*, 1877–1880, 2007.
18. Jing, P. and R. Ziolkowski, "Metamaterial inspired, electrically small huygens sources," *IEEE Antennas and Wireless Propagation Letters*, Vol. 9, 501–505, Jun. 2010.
19. Best, S., "Progress in the design and realization of an electrically small Huygens source," *IEEE International Workshop on Antenna Technology, iWAT*, 1–4, 2010.
20. Senturq, B., A. Sharaiha, and S. Collardey, "Superdirective metamaterial-inspired electrically small antenna arrays," *European Conference on Antennas and Propagation, EUCAP*, 151–155, Gothenburg, Sweden, Apr. 2013.
21. Busch, K., G. von Freymann, S. Linden, S. F. Mingaleev, L. Tkeshelashvili, and M. Wegener, "Realization of negative-index materials," *Physics Reports*, Vol. 444, 101, 2007.